Environ Earth Sci (2016) 75:322
DOI 10.1007/s12665-015-5128-6

ORIGINAL ARTICLE

# The hermitage of Cerbaiolo (Tuscany, Italy): stability conditions and geomorphological characterization

**Laura Melelli[1] · Corrado Cencetti[1] · Manuela Cecconi[2] · Luciano Faralli[3] · Alessia Vecchietti[2] · Vincenzo Pane[2]**

Received: 16 January 2015 / Accepted: 1 October 2015 / Published online: 11 February 2016


**Abstract** The Italian cultural heritage is one of the most noticeable in the world; an important part of it is subjected to natural hazard and risk conditions. Religious buildings, due to their location on impervious sites are particularly exposed to landslides. In this paper we study the hermitage of Cerbaiolo (Tuscany, central Italy). The hermitage, founded in the 8th century as a Benedictine monastery is now a Franciscan Women Institute seat. The buildings are on the edges of a limestone plate overlapped to a clayey formation. Falls, toppling and slides are present along the limits of the plate due to the geomechanics properties of the rock and to the contrast between the two lithological complexes. In order to identify the main joint sets affecting the rock mass a structural-geological survey was carried out and four sets are identified. The rock plate was classified according to Bieniawski, Barton and Geological Strength Index approaches. The outcomes confirm the predisposing factors to mass movements, corresponding to the intensity and characteristics of fracturing of the rock mass. With regard to the slope stability analysis, a failure mechanism involving sliding along a single plane (plane failure) was assumed on the first approximation. The analyses take into account the presence of tension cracks as an indicator factor for the instability phenomenon. The results of stability analyses, performed in static and seismic conditions, indicate a widespread instability condition. The dip slope direction, the properties and type of discontinuities and the local variation of composition influence the hazard assessment.

**Keywords** Cultural heritage · Geomorphology · Rock mass characterization · Slope stability · Tuscany

## Introduction

Italy has one of the most noticeable world cultural heritages, but the Italian territory is also prone to natural hazard. Landslides, flooding, earthquakes and volcanic activity are the most widespread causes of natural risk for national heritage. In particular, the 6.6 % of the cultural heritage is subjected to landslides and the 11.7 % to floods (Spizzichino et al. 2013).

In the past, cultural heritage of religious architecture was placed in inaccessible places. In most cases, hermitages are typically located on the edge of vertical cliffs, or on the top of small plates (Margottini et al. 2015), in order to assure the necessary protection and isolation for the religious people who lived there. In some cases, the monasteries are built into the rock mass for a significant part of the structure (D'Amato Avanzi et al. 2006). These characteristics are common to different geographical and cultural contexts, from South America with the famous site of Machu Picchu (Canuti et al. 2005; Casagli et al. 2005) to the Asian continent and the Buddha niches in Afghanistan (Margottini 2001). The most numerous examples are in Europe (Margottini et al. 2015), because of the many ancient civilizations that populated the Mediterranean basin. Due to such impervious locations, the most frequent natural hazard is represented by landslide events (Marinos

✉ Laura Melelli
laura.melelli@unipg.it

[1] Dipartimento di Fisica e Geologia, Università di Perugia, Perugia, Italy

[2] Dipartimento di Ingegneria, Università di Perugia, Perugia, Italy

[3] S.G.A. Studio Geologi Associati, via XX Settembre 76, Perugia, Italy

et al. 2002; Marinos and Tsiambaos 2002; Marinos and Rondoyanni 2005; Taboroff 2000; Lollino and Pagliarulo 2008; Tanarro and Muñoz 2012; Bednarczyk 2015; Laskowicz and Mrozek 2015). Falls and slides are the most frequent types of landslide, but debris flows and sites involved in aggradation of alluvial fans are also present (McCahon et al. 2001). The concept of protection and preservation of the cultural heritage has been introduced by the UNESCO Convention (1972), whereas the landslide risk is one of the key issues of the International Programme on Landslides (Sassa 2004a, b). With the aim of analyzing the best practical preservation approaches, several methods of investigation have been proposed. The monitoring and the modeling of slope instability is the most recurrent approach (Fanti et al. 2013).

Tuscany (central Italy) shows noteworthy examples of ancient religious sites affected by natural hazard, in particular landslides, since they are commonly located in mountain areas (Borgatti and Tosatti 2010), as for example the Calomini hermitages in Garfagnana (D'Amato Avanzi et al. 2006) or La Verna monastery (Canuti et al. 1993). In some cases, the particular geological setting made of hard and fractured limestone plates overlapping soft clays is the main factor triggering mass movements. This geological setting is also widespread in large areas of the northern Apennines. The Val Marecchia rock slabs offer the most important examples (Spreafico et al. 2015): the natural hazard affecting the Pietra di Bismantova (Borgatti and Tosatti 2010) or the San Leo cliff (Ribacchi and Tommasi 1988; Nesci et al. 2005) are interpreted as deep seated gravitational slope deformations (DSGSDs), which are a type of lateral spreads (Dramis and Sorriso-Valvo 1994; Benedetti et al. 2013; Bozzano et al. 2013). The presence of rigid slabs over ductile rocks induces the spreads over a localized shear zone. Although the DSGSD is the main factor for the instability of the area, single and different mass movements occur both in the plate and in the basal sediments. Along the edge of the rock plate, falls, toppling and rockslides occur whereas flows and slides involve the basal clays. If the evolution of the DSGSD is slow and intermittent, the landslides occurring in the zone between the two lithological complexes are recurrent and rapid. DSGSD are, therefore, the most important events in terms of hazard and risk assessment.

In this paper we have analyzed the case history of the Cerbaiolo hermitage (Arezzo, Tuscany, Melelli 1998; Candio et al. 2000). The building has its foundations on a man-made terrace located on the edge of a steep rock plate. Moreover, along the rear perimeter the building rests on the rock. In some places the rock replaces the walls, thus becoming part of the building itself.

The hard and fractured rock rises on the underlying gentle slopes. The geological and geomorphological parameters are relevant predisposing factors for slope instability, which is caused by the contrast between the two lithological complexes. In fact, both the load transferred from the rock mass and the tensile stress on the plate below induce evident damage on the building.

The results of the geomorphological assessment, supported by the analysis of a high resolution digital terrain model (HR DTM) are presented in the paper. Moreover, a rock mass classification and a plane failure analysis are proposed. We show that the approach presented in this paper provides a complete framework for the planning of possible technical solutions aimed to slope safety.

## The hermitage of Cerbaiolo: geological and geomorphological assessment

The hermitage of Cerbaiolo (Lat. 4,840,067.72 Long. 1,748,977.42, 861 m a.s.l. Tuscany, Italy) stands on the limit of a rock plate, overlooking southward the Upper Tiber Valley and the Montedoglio Lake (Fig. 1).

The hermitage was founded in the 8th century as a Benedictine monastery; between 1216 and 1783, Franciscan friars were hosted. During the World War II, the entire buildings were destroyed; thereafter the hermitage was totally restored and since 1967 became the seat of Franciscan Women Institute. The building plan is similar to the configuration of a 17th century cloister, enclosed by the church, the sacristy, the refectory, the chapel and the cells. Three stone altars from the Renaissance period are preserved in the church, embellished with 18th century portals and a polygonal apse. Focus of interest is the Chapel of Sant'Antonio, a tower building dated 1716 with the western side leaning and touching the bedrock. Presently, the hermitage hosts pilgrims for religious retreats. Cerbaiolo is included in the Italian Cultural Heritage ("Carta del Rischio del Patrimonio culturale") realized by ISCR (Central Institute for the Conservation and Restoration, http://www.cartadelrischio.it). The area around the Cerbaiolo hermitage is mapped in the database as prone to seismic risk. Nevertheless, the most important hazard is related to the slope instability conditions affecting the bedrock.

The rock plate has an elliptical shape, elongated in a NNE–SSW direction and covering an area of 0.2 $km^2$, which is entirely surrounded by gentle slopes (Fig. 2a).

The altitude values range between 874 and 717 m a.s.l. The geomorphological and morphometric assessment is supported by LiDAR (Light Detection And Ranging) data (downloadable from http://www502.regione.toscana.it/geoscopio/cartoteca.html). The Digital Terrain Model (DTM) has a cell size equal to 10 × 10 m. The plate dips toward NE; therefore, the southern margin where the hermitage is settled is a section with higher difference in

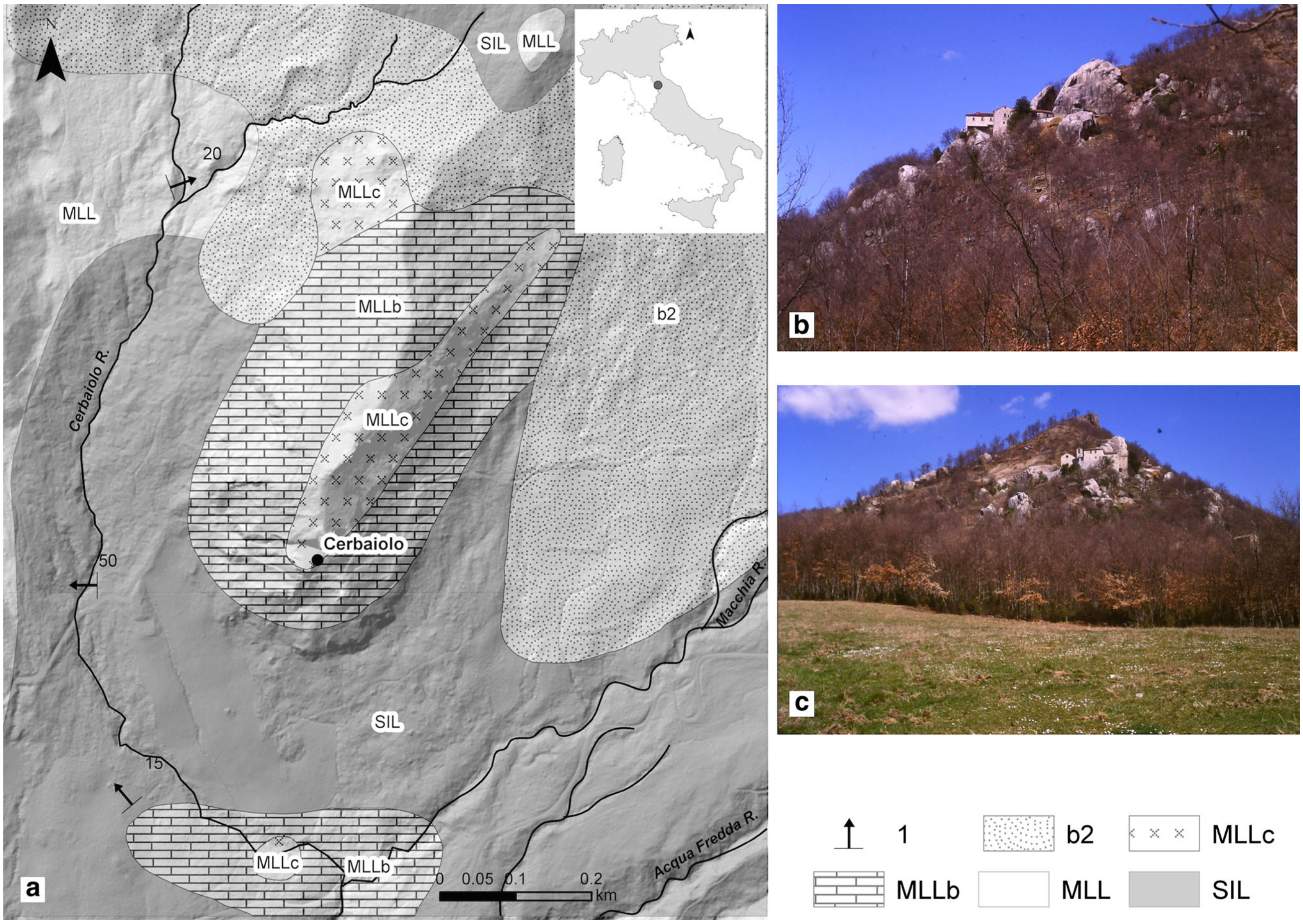


**Fig. 1** Location map of the study area. **a** Geological map and location plan of the study area. **b** The hermitage of Cerbaiolo, view from the east and **c** from the south. *1* Strike and dip symbol of layers. The number is the angle of dip, *b2* eluvial and colluvial deposits, MLLc) Breccia di basalto (basalt cemented gravel), *MLLb* Breccia di Cerbaiolo (Cerbaiolo's cemented gravel), *MLL* Monte Morello formation (Lower—Middle Eocene), *SIL* Sillano formation (upper Cretaceous/lower-middle Miocene)

altitude with respect to the basement below the plate. Only the 14 % of the plate area shows slope values higher than 40°, with a well define spatial arrangement (Fig. 2a): the highest slope values are grouped along the southeastern portion. In particular, on the southern side, the slope increases along well-defined scarps, with a meaningful continuity in plan. The aspect distribution (Fig. 2b) highlights a shape of the plate similar to an irregular tetrahedron with the smallest face towards the South direction and two sides elongated on the opposite direction, NW and SW, respectively. The basement below the plate shows medium gentle slopes with values around 14°. The resulting landscape, with high escarpments abruptly connected with the flat areas above, is strictly related to the geological and geomorphological setting.

In the study area two lithotypes crop out (Fig. 1), included in the Ligurian units, geometrically overlapping both the Umbria-Marche-Romagna Unit and the Tuscany one (Bettelli and Panini 1991; Cerrina Feroni et al. 2002). The Ligurian units are the uppermost ones of the entire Apennine nappe pile, thrusting from West to East. The two lithotypes are very different in terms of response to geomorphological processes. From the bottom to the top, the gentle hilly area with low slope values around the plate is occupied by the Sillano formation (upper Cretaceous/Lower-Middle Miocene—Bortolotti 1962; Bortolotti et al. 2008). The formation is heterogeneous, consisting of very irregular alternation of shales, siltstones, sandstones, limestones and marly limestones, and rare calcarenites. The shales, dark grey, brown and sometimes reddish or greenish, usually constitute the main part with layers of very variable thickness. The deposits are related to pelagic environment of turbiditic basin. The formation is deformed due to the tectonic stress responsible for putting in place the overlap of the Ligurian unit. Due to the strong deformation is not possible to define the thickness, which is estimated around 100–150 m. The contact with the overlying Mt. Morello formation is always tectonic.

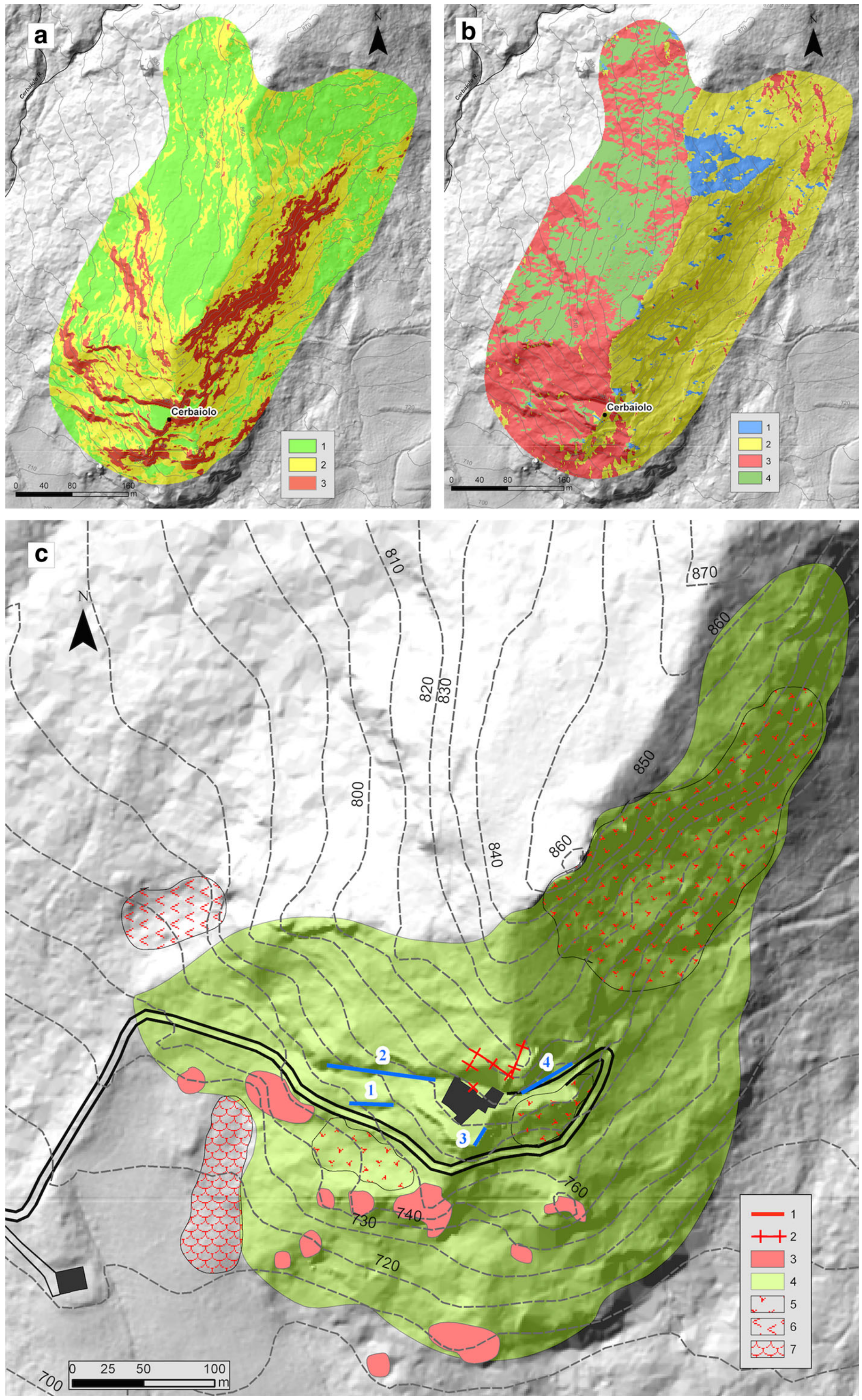


**Fig. 2** Topographic attributes characterizing the rock plate of Cerbaiolo (Monte Morello formation). **a** slope values, *1* 0°–23°, *2* 23°–40°, *3* >40°. The class 1 cover the 46 %, the class 2 the 40 % and the class 3 the 14 % of the total area. **b** aspect values, *1* 0°–90°, *2* 90°–180°, *3* 180°–270°, *4* 270°–360°. **c** Geomorphological features. *1* Measurement station, *2* trench, *3* isolated block, *4* area affected by falls and topples, *5* debris, *6* slide, *7* flow

The Mt. Morello formation (Lower—Middle Eocene) constitutes the entire plate where the hermitage is founded (Bortolotti 1962; Ponzana 1993; Bortolotti et al. 2008). The formation shows an irregular repetition of calcareous marls and sandstones of highly variable thickness and extension. The deposits can be attributed to a turbiditic facies in a deep-sea environment. At the base or within the lower part of the formation, as well as in the examined area, large volumes of mono or polygenic debris are present with thickness from a few tens to hundreds of meters. Olistoliths together with ophiolitic material of kilometric size are also present. In particular, the rocky spur, on which the hermitage rises, is made up of two units: the MLLb, named “Breccia di Cerbaiolo” (Cerbaiolo’s cemented gravel) at the base, and the MLLc or “Breccia di basalto” (basalt cemented gravel) on the top. MLLb and MLLc are interpreted as olistostromes, due to large submarine landslides triggered on the front of the Ligurian Units progressing towards northeast.

MLLb is lacking of micrite; decimetric clasts with sharp edges of “Calcari a Calpionelle” (Calpionelle Limestones) and a rich microfauna characterize—the unit with Calpionellidi (*Calpionella alpina*, *C. elliptica*, *C. cf. undelloides*, *C. massutiniana*, *Calpionellopsis cf thalmanni*, *Stenosemellopsis cf. hispanica*, *Tintinnopsella oblonga*, *T. doliphormis*). Rare fragments of basalt and jasper are also observed. MLLc is formed by grain-supported grainstones with basaltic fragments locally forming the fine sandy loam matrix, rare clasts of jasper and limestone. On the bedrock, colluvial deposits are locally present. Near the hermitage the bedrock is organized into thick layers dipping NW, locally intercalated with clayey silt levels. The area is tectonically and morphologically active as confirmed by the seismic activity and by the morphological and morphometric parameters, which are well evident in the southeast quaternary Upper Tiber basin (Delle Donne et al. 2007; Melelli et al. 2014; Pucci et al. 2014).

## Slope stability conditions

The boundary conditions affecting the slope stability (Fig. 2c) are the:

- Contrast between the mechanical properties of the two lithological units;
- Degree of rock fracturing that decreases from the edges towards the center of the plate. Up to an altitude of 825 m a.s.l. towards northwest, fractures are not evident. On the contrary, above this altitude and along the southern portion of the plate (in particular near the contact with the basal clays) fractures are common and frequent;
- Filling of some fractures consisting of clayey silts,
- Layers attitude. Along the western flank strata show a dip slope direction; on the contrary, on the opposite side of the plate, the anti-dip slope direction prevails,
- Circulation of underground water, in particular along the contact between the plate and the basement,
- Karstic activity inside the calcareous plate, induced also from the open fractures pervading the rock mass.

The western flank is involved in occasional slides due to the dip direction of the massive blocks. On the eastern flank, the lower degree of fracturing promotes the block debris accumulation at the foot of the plate. The clasts have sizes of several decimeters. The southern sides, where the buildings are placed, offer the most complex condition for slope stability.

Gravity induced erosion scarps and block debris are present at the base of the scarps. On the top of the plate trenches are visible, which confirm the tensional forces acting on the hard rocks. The main part of these fractures is open, confirming that the movement progression is more rapid than the filling activity. The intersection of the discontinuities is the cause for the toppling, falling and sliding of several blocks. The volumes range from 10 to about 200–220 $m^3$.

The distance covered by the blocks is estimated to be up to 400 m. In some cases, the groups of discontinuities measured along the southern front show a rotation towards SE of about 15°/20° due to the slow downslope sliding.

The Sillano Formation is involved in the flows (Fig. 2c) triggered by the fluvial erosion at the foot of the slope. Two main streams with a moderate erosional activity are presently delimiting the area: the Cerbaiolo stream flowing along the western boundary from north, and the Macchie stream from NE.

The entire plate has been interpreted as affected by lateral spreads (Nemcok 1972; Melelli 1998), due to the predisposing conditions of a thickly bedded sequence of hard rock overlying soft sediments with a strong rheological contrast. The absence of a well-defined sliding surface, the tensile landforms on the edge of the plate and the movement downslope of isolated blocks (southern portion) confirm this.

The area surrounding Cerbaiolo is included in the Italian Landslide Inventory (IFFI Project—“Inventario dei Fenomeni Franosi in Italia”, i.e. Landslides Inventory in Italy) developed by ISPRA (Italian National Institute for Environmental Protection and Research), thus confirming the rock fall and toppling in the southern portion and the flows in the basal clays.

In summary, the slope stability conditions of the plate are different considering kinematics and evolution in the three main slope sides; several shallow landslides may be recognized, but the entire hard bedrock superimposed on the soft clays is interpreted as affected by a DSGSD type of lateral spreads.

## Rock mass characterization

In order to identify the main families of discontinuities that affect the rock mass, data were collected from four stations where a structural-geological survey was carried out (Figs. 2c, 3).

The analysis was concentrated along the walls next to the buildings, as they are more representative for the

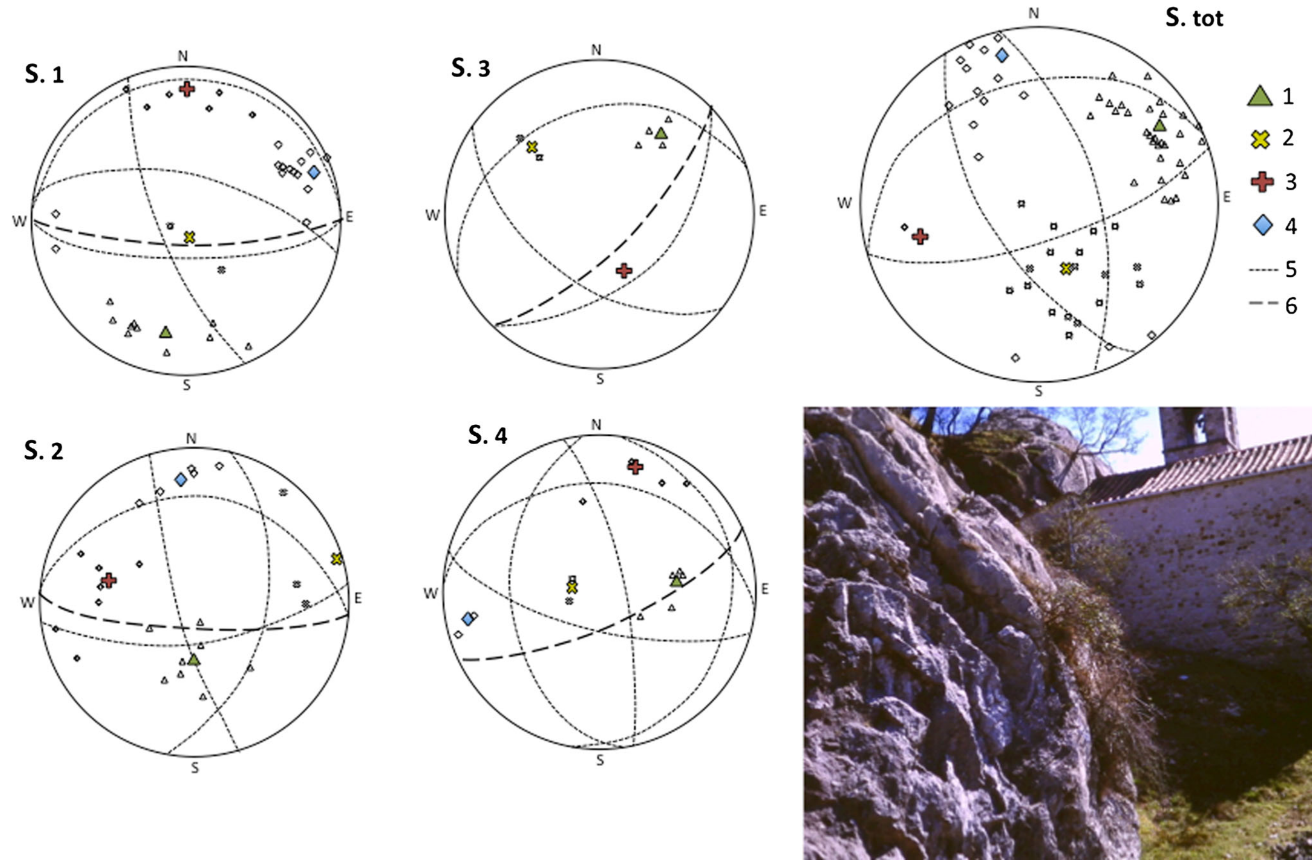


**Fig. 3** Stereonets displaying the data collected in the measurement stations (from *S.1* to *S.4*) and the entire dataset (*S. tot*). The numbering of the stations is referred to Fig. 2c. In the photo the mass rock along the southern edge of the plate with the location of the measurement station n. 1. *1* 238°/65°, *2* 344°/33°, *3* 73°/65°, *4* 162°/71°, *5* great circle of each group of discontinuities, *6* great circle of the slope with the measurement stations

assessment of the risk affecting the hermitage. Three of the four stations are located along the southern side; the fourth is located on the southeast side.

From the data collected on all fronts, four main families of discontinuities were individuated (Fig. 3), attitude (average values in degree for azimuth and dip):

1. 238°/65°,
2. 344°/33°,
3. 73°/65°,
4. 162°/71°.

In order to characterize the rock mass according to standard procedures (ISRM 1993), the following data for each family of discontinuities of each station were collected: type of discontinuity and its orientation; spacing; persistence; roughness; aperture; filling.

The average values were used to classify the rock mass according to the classifications of Barton et al. (1974), Bieniawski (1989) and Marinos and Hoek (2000). Table 1 shows the partial indices and the corresponding parameters assigned to the rock in every station for the different families of discontinuities.

Generally, fractures occur as joints; the discontinuities with inclination close to the horizontal have to be considered as layering and they are not very common, due to the considerable thickness of the limestone strata.

The spacing is mostly between 0.6 and 2 m; most of discontinuities show a remarkable linear persistence that, from available observation points, appears to continue even inside the rock mass. In detail, the discontinuities have a slightly wavy plan: the roughness of the fractures, as measured by the Barton's comb and reported according to profiles of roughness defined by Barton, is between Class 6 and Class 7 (10–12 < JRC < 14–16). The opening is extremely variable and shows values >0.5 cm, with some very high values, even up to 2 m. Even filling is strongly differentiated, in terms of quantity and type of material. The fractures that are not filled or that are filled by secondary calcite are very rare; in most cases, this is silty or silty-sandy material transported and deposited by runoff. During the field survey, the fractures appeared completely dried. Only one spring was detected, along the access road to the hermitage, with values of discharge almost constant, ranging between 20 and 30 l/min. Despite of this, there is

**Table 1** RMR Index calculated in four stations on the plate of Cerbaiolo hermitage in order to determine the quality of rock mass

| Bieniawski | Station 1 | | Station 2 | | Station 3 | | Station 4 | |
|---|---|---|---|---|---|---|---|---|
| Rebound (*R*) | 60.6 | | 57.1 | | 58.4 | | 70.1 | |
| Unit volume weight (kN/m$^3$) | 23 | | 23 | | 23 | | 23 | |
| $\sigma_c$ (MPa) | 68.3 | | 65.6 | | 66.6 | | 75.6 | |
| A1 | **7** | | **7** | | **7** | | **8** | |
| RQD (%) | 100 | | 100 | | 100 | | 100 | |
| A2 | 20 | | 20 | | 20 | | 20 | |
| *S* (m) | $0.6 < S < 2$ | | $S > 2$ | | $0.6 < S < 2$ | | $0.6 < S < 2$ | |
| A3 | 15 | | 20 | | 15 | | 15 | |
| JRC | 12 | Partial index 4 | 12 | Partial index 4 | 14 | Partial index 5 | 10 | Partial index 4 |
| Ap (mm) | >5 | Partial index 0 | >5 | Partial index 0 | >5 | Partial index 0 | >5 | Partial index 0 |
| q/JCS | Not or lightly altered | Partial index 6 | <1.5 | Partial index 6 | <1.5 | Partial index 6 | <1.5 | Partial index 6 |
| Filling | Compact | Partial index 2 | Uncohesive | Partial index 2 | Uncohesive | Partial index 2 | Uncohesive | Partial index 2 |
| Persistence | Persistence 45 ÷ 90 % | Partial index 2 | Persistence 45 ÷ 90 % | Partial index 2 | Persistence 45 ÷ 90 % | Partial index 2 | Persistence 45 ÷ 90 % | Summa of partial indexes |
| A4 | 14 | | 14 | | 15 | | 13 | |
| Hydraulic conditions | Dry | | Dry | | Dry | | Dry | |
| A5 | 15 | | 15 | | 15 | | 15 | |
| Ic (compensation coefficient for slopes) | 2 directions | Unfavorable | 2 directions | Unfavorable | 1 direction | Fair | 1 direction | Fair |
| Ic | 50 | | 50 | | 25 | | 25 | |
| RMR | 21 (IV class) | | 26 (IV class) | | 47 (III class) | | 46 (III class) | |

*Co* cohesion, *RQD* rock quality designation, *S* spacing, *JRC* joint roughness coefficient, *Ap* aperture, *JCS* joint compressive strength

no doubt that, in the case of exceptional weather events, a water circulation inside the discontinuity and a saturation of the filling material can occur because of the presence of fractures that commonly intercept the ground level.

As for the classification of the rock mass according to the criteria of Bieniawski, we applied a compensation coefficient for slopes under "unfavorable" conditions (i.e. with at least two critical directions, identified by the stereonets). The rock mass, according to Bieniawski, has a value of RMR between 20 and 55; therefore, its quality ranges from poor to fair (Table 1).

According to Barton's classification (Table 2), using the same parameters, the rock mass has a *Q* index between 0.58 (based on data collected on three fronts) and 0.73 thus belonging to the range of the class with quality "very poor" (VII class).

For the classification of the rock mass according to the Hoek's criteria, we used a correlation between the structural characteristics of the rock mass, in terms of degree of fracturing and tectonic disturbance, and the characteristics of the surfaces of discontinuities, in terms of roughness, alteration and filling.

The rock mass has a GSI between 51 and 59, estimated in the four stations.

The results confirm the presence of predisposing factors to mass movements, represented by the intensity and characteristics of fracturing of the rock mass.

## Plane failure analyses

The stability of sub-vertical rock wedges has been carried out assuming plane failure conditions. The rock mass characterization described in "Rock mass characterization" section, and already cited in Candio et al. (2000), allows us to assume for the calcareous cliff—and on first approximation—a failure mechanism involving sliding

**Table 2** Classification of rock mass according to Barton's criterion

| BARTON | Station 1 | Station 2 | Station 3 | Station 4 |
|---|---|---|---|---|
| RQD (%) | 100 | 100 | 100 | 100 |
| Jn | 15 | 15 | 12 | 15 |
| Jr | 3 | 3 | 3 | 3 |
| Ja | 5 | 5 | 5 | 5 |
| Jw | 1 | 1 | 1 | 1 |
| SRF | 7.5 (D) | 7.5 (D) | 7.5 (D) | 7.5 (D) |
| RQD/Jn | 6.67 | 6.67 | 8.33 | 6.67 |
| Jr/Ja | 0.60 | 0.60 | 0.60 | 0.60 |
| Jw/SRF | 0.13 | 0.13 | 0.13 | 0.13 |
| *Q* | 0.52 | 0.52 | 0.65 | 0.52 |

*RQD* rock quality designation, *Jn* joint set number, *Jr* joint roughness number, *Ja* joint alteration number, *Jw* joint water reduction factor, *SRF* stress reduction factor, *Q* quality index

along a single plane, which shows a dip ($\psi_p$) which is smaller than the dip slope face ($\psi_f$). The presence of tension cracks and discontinuities hidden in the rock mass and different hydraulic conditions have been examined to account for cleft pressures. Several stability analyses have been performed in static and seismic conditions.

The geometry of the slope considered in the analysis is defined in Fig. 4a, b). The slope may have a vertical tension crack in its upper face. The sensitivity of the factor of safety of a slope of given height and face dip to the position of the tension crack and to the dip of the failure plane, was examined in the two limit water conditions (Cecconi and Viggiani 2000) of "dry" slope ($z_w/z = 0$) and "wet" slope ($z_w/z = 1$).

The general expression of the safety factor of the slope, $F$, given by the ratio of total forces resisting sliding to the total forces tending to induce sliding, considering a Mohr–Coulomb failure criterion along the discontinuities, can be expressed in static conditions as (Wyllie and Mah 2004):

$$F\left(\frac{z}{H}, \psi_p\right) = \frac{2N \times P + \left(\frac{Q}{\tan\psi_p} - R \times (P + S)\right)\tan\varphi}{Q + \frac{RS}{\tan\psi_p}} \tag{1}$$

where $N$, $P$, $Q$, $R$ and $S$ are non-dimensional quantities defined as follows:

$$\begin{aligned} N &= \frac{c'}{\gamma H};\ P = \left(1 - \frac{z}{H}\right) \times \frac{1}{\sin\psi_p}; \\ Q &= \left(\left(1 - \frac{z^2}{H^2}\right) \times \frac{1}{\tan\psi_p} - \frac{1}{\tan\psi_f}\right) \times \sin\psi_p \\ R &= \frac{\gamma_w}{\gamma}\frac{z_w}{z}\frac{z}{H};\ S = \frac{z_w}{z}\frac{z}{H}\sin\psi_p \end{aligned} \tag{2}$$

In Eq. (1), the ratio *z/H* relative to the position of the tension crack and the failure plane inclination, $\psi_p$, can be regarded as slope stability indicators. For a dry slope, since $R$ and $S$ are both zero, the factor of safety is only a function of the tension crack depth and the dip of the failure plane and Eq. (1) simplifies into:

$$F\left(\frac{z}{H}, \psi_p\right) = 2N \times \frac{P}{Q} + \frac{\tan\varphi}{\tan\psi_p} \tag{3}$$

The analysis has been first carried out considering a simplified geometry, representative of the Cerbaiolo rock slope, which is a dry calcareous rock slope with a height, $H = 5$ m, and an average dip slope face, $\psi_f = 80°$. Based on the rock mass characterization (see "The hermitage of Cerbaiolo: geological and geomorphological assessment" section), it has been assumed $\gamma = 23$ kN/m$^3$. As for the strength parameters along the sliding surface, we consider a plausible range of values for the friction angle, $\phi' = 25°$, 30°, 35° and cohesion $c'$ values not exceeding 50 kPa.

The factor of safety given by Eq. (3) is represented in Fig. 5a as a function of *z/H* and $\psi_p$. The absolute minimum of the factor of safety (for static conditions) has been analytically found by differentiating $F(z/H, \psi_p)$ with respect to both *z/H* and $\psi_p$ and equating the resulting differentials to zero. This yields $F_{min} = 0.825$ for $\psi_p \cong 48°$ and $z/H \cong 0.55$, when $\phi' = 30°$ and $c' = 10$ kPa. On the other hand, following Wyllie and Mah (2004), for any given value of $\psi_p$, the minimum value (relative) of $F$ can be found by differentiating Eq. (3) with respect to *z/H*, thus leading to the following critical value of *z/H*:

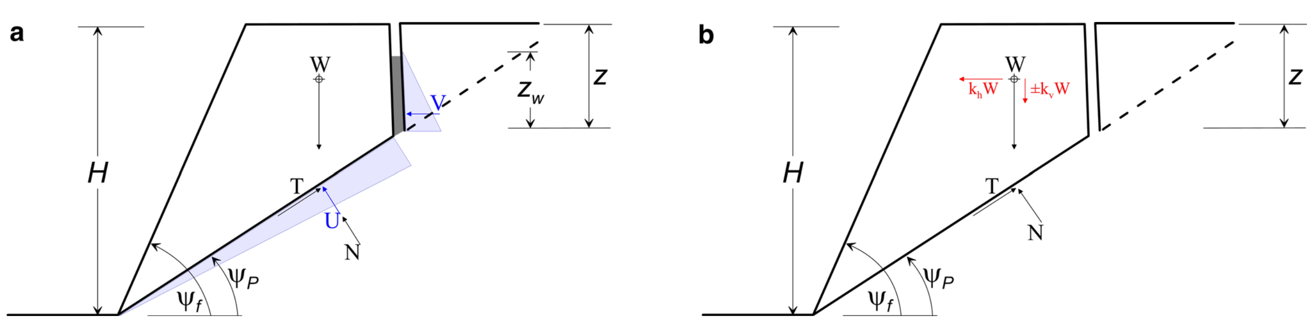


**Fig. 4** Slope geometry for plane failure: **a** general case in static conditions; **b** seismic case and pseudostatic forces

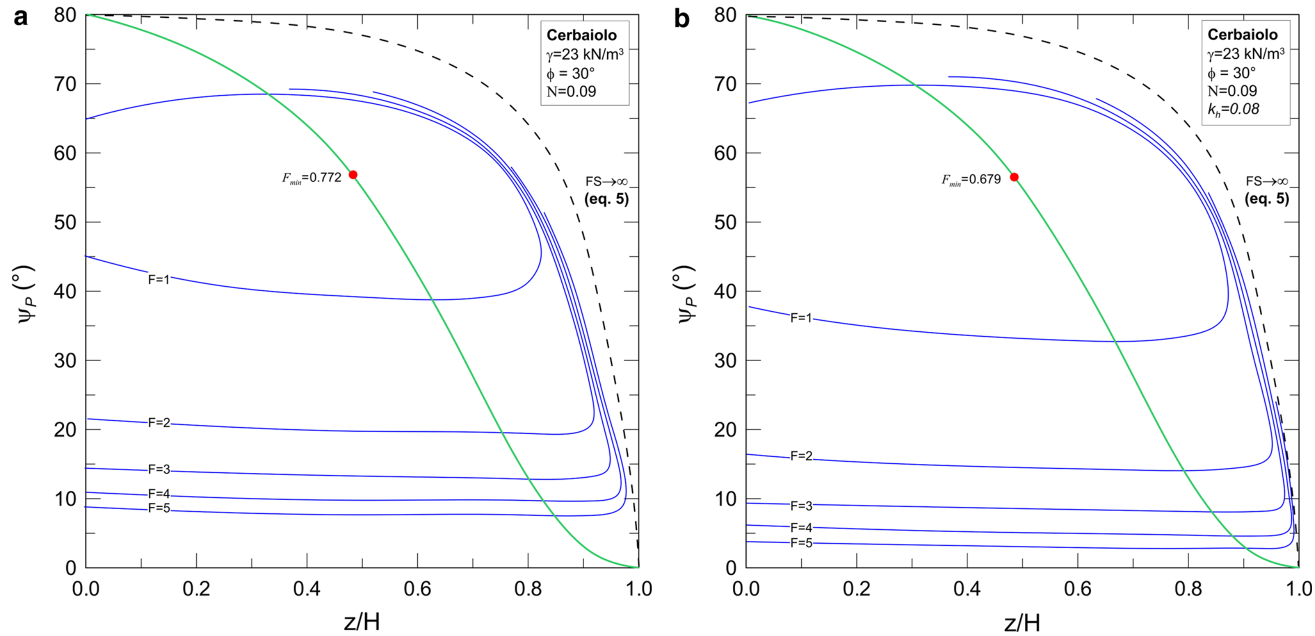


**Fig. 5** Rock slope stability analysis at Cerbaiolo in dry conditions: $F$ contours for $H = 5$ m, $\psi_f = 80°$: **a** static, **b** seismic conditions

$$\frac{z}{H} = 1 - \sqrt{\frac{\tan\psi_p}{\tan\psi_f}} \tag{4}$$

which is represented by the dashed curve in Fig. 5a ($\psi_f = 80°$). According to Eq. (3), another limit condition may occur when $Q = 0$, i.e.

$$\frac{z}{H} = \sqrt{1 - \frac{\tan\psi_p}{\tan\psi_f}} \tag{5}$$

Starting from Eq. (3), the equation defining the factor of safety for the seismic conditions has been derived through a pseudostatic approach as follows:

$$F\left(\frac{z}{H}, \psi_p, k_h\right) = \frac{2N \times P + Q \times \left[\frac{(1+k_v)}{\tan\psi_p} - k_h\right] \tan\varphi}{Q \times \left[(1+k_v) + \frac{k_h}{\tan\psi_p}\right]} \tag{6}$$

In Eq. (6), $k_h$ is the horizontal seismic coefficient and $N$, $P$, $Q$ are the same non-dimensional quantities defined in Eq (2) and $k_v = \pm 0.5\ k_h$.

The seismic input parameters for the Cerbaiolo site ($a_g = 0.221$ g) are listed in Table 3; for this site, in accordance with the Italian National Code (DM 2008), the horizontal seismic coefficient is:

$$k_h = \beta_s \times S \times \frac{a_g}{g} \tag{7}$$

where $S$ is the amplification factor ($S = S_S S_T = 1.2$, see Table 3).

In seismic conditions, the absolute minimum of the factor of safety ($F_{min}$) has been calculated analytically, by differentiating $F(z/H, \psi_p)$ with respect to both $z/H$ and $\psi_p$ (see Fig. 5b). The obtained results are $F_{min} = 0.679$ for $\psi_p \cong 57°$ and $z/H \cong 0.48$, when $\phi' = 30°$ and $c' = 10$ kPa.

The influence of groundwater on the stability of the rock slope has been also assessed, assuming that water enters the failure surface through the tension crack and seeps along the former, according to a linear distribution of water pressures reducing to the atmosphere at the toe of the slope, as shown schematically in Fig. 4a for the static case.

The relationship between the dip of the sliding surface, $\psi_p$, and the critical ratio $z_w/H$, when the tension crack is entirely filled with water ($z_w/z = 1$), can be obtained solving Eq. (1) by posing $F = 1$. Figure 6a shows the *iso-F = 1* curves obtained for $H = 5$ m, $\psi_p = 80°$ and different values of friction angle, $\phi'$ (25°–35°) and cohesion, $c'$ (10–50 k Pa). The results show that the critical ratio $z_w/H$ ($\equiv z/H$) decreases with increasing dip of the sliding surface, $\psi_p$, till it reaches a minimum value and then it increases again. The value of $\psi_p$ at which $z_w/H$ is minimum does not depend on cohesion, and it is attained approximately at $\psi_p \cong 60°$. Figure 6b describes a more general result, showing the *iso-F = 1* curves obtained for increasing values of non-dimensional group $N$, thus including varying values of $\gamma$, $H$, and cohesion, $c'$.

Motivated by these results we performed a parametric study in order to investigate the effects of rock mass geometry (slope height, $H = 3$, 5, 8 m) and strength parameters of the material coating the joint surface ($c' = 10$, 30, 50 kPa; $\phi' = 25°$, 30°, 35°) on the stability conditions, in both static and seismic cases. A further set of stability analyses has been then performed (see Table 4).

**Table 3** Seismic input parameters for the site of Cerbaiolo (Pieve Santo Stefano, Arezzo, Italy)

| Cerbaiolo (Arezzo, Italy), Lat. 43,672,671, Lon. 12.089067 WGS84 ($T_R = 475$ years) | |
|---|---|
| $a_g$ (g) | 0.221 |
| $F_0$ | 2.342 |
| $T_C$*(s) | 0.303 |
| Ground type A, $S_S S_T$ | 1.2 |
| $k_h = \beta_s\, a_{max}/g$ | 0.08 |

The results of such analyses are shown in Fig. 7a, b—static and seismic conditions, respectively—in terms of minimum (absolute) safety factor, $F_{min}$, as a function of the rock slope height, $H$. When considering values of $H$ larger than 3 m, a critical condition could be achieved if effective cohesion is smaller than about 10 kPa. Of course, this situation appears even worst when the seismic actions are taken into account (Fig. 7b). As expected, an increase of soil friction angle is favourable in both situations.

The solutions of safety factor, achieved for $c' = 0$ are plotted in Fig. 7c, as a function of dip failure plane ($\psi_p$), since they do not depend on $H$ but, rather, on friction angle ($\phi$) only. In particular, for the seismic case, when $c' = 0$, Eq. (6) reduces to:

$$F(k_h, \psi_p) = \frac{\left[(1 + k_v) - k_h \tan\psi_p\right] \tan\varphi}{\left[(1 + k_v)\tan\psi_p + k_h\right]} \quad (8)$$

Another way to enhance the effect of cohesion $c'$ is shown in Fig. 8a, b. Here, the *iso-F* = 1 curves are plotted for increasing values of cohesion. In static conditions, the minimum value of cohesion which guarantees $F = 1$ is $c' = 16$ kPa and contextually, $\psi_p = 55°$, $z/H = 0.5$. Effective cohesion $c'$ lower than this value may yield to safety factors smaller than unity depending on $\psi_p$ and $z/H$. For example, point 1 falls on a region denoting a safe situation if $c' \geq 15$ kPa with $\psi_p = 50°$ and $z/H = 0.32$. Provided that $c' \geq 15$ kPa, point 2 is also representative of a stable rock mass with a same dip failure plane, $\psi_p = 50°$, but $z/H \cong 0.7$. On the other hand, point 3 denotes an unstable condition for values of $c' < 5$ kPa. When seismic actions are considered, the minimum critical value of $c'$ is about 20 kPa, whereas $\psi_p = 52°$, $z/H = 0.54$. The case study of Cerbaiolo ($\phi = 30°$, $\psi_p = 65°$, $\psi_f = 80°$) is once more plotted in Fig. 8a, b), highlighting an observed unstable situation of the calcareous rock mass, consistently with values of cohesion smaller than $c' = 10$ kPa.

## Summary and conclusions

Ancient sites of religious architectures are widespread on the Italian territory. They are often located in impervious sites because of the necessary isolation and protection they require, and this often implies that these sites are subjected to natural hazard, mainly represented by landslides, which create risk conditions for both the religious living inside the buildings and the pilgrims visiting the sites.

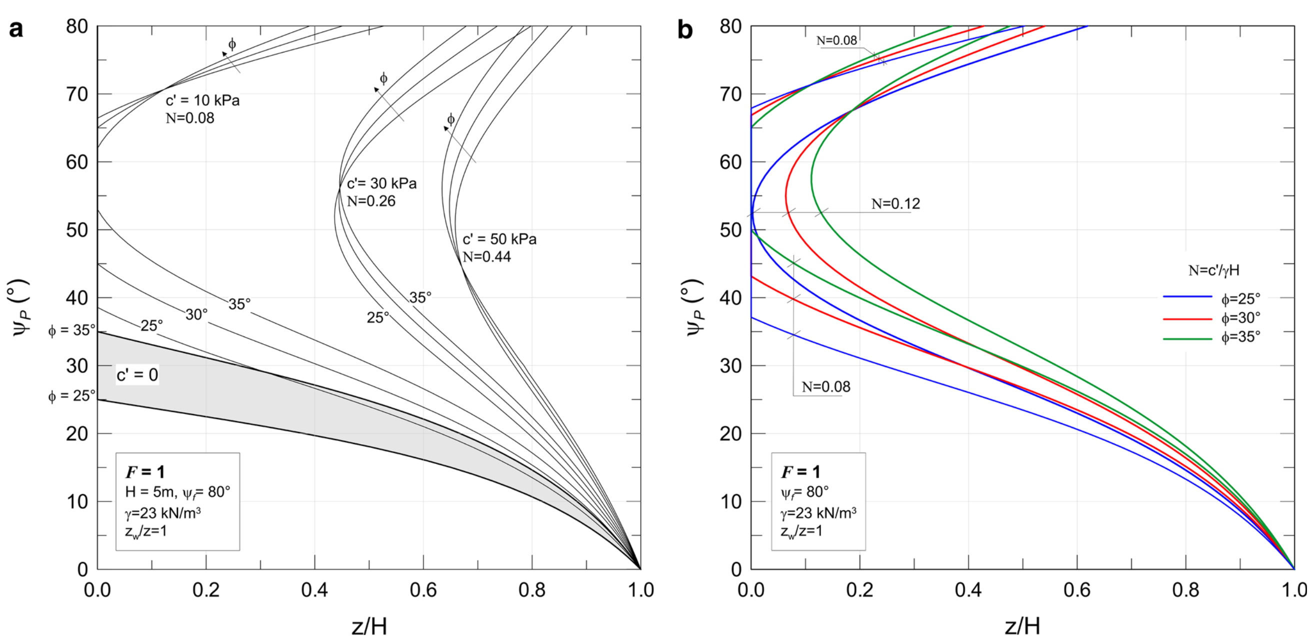


**Fig. 6** Rock slope stability analysis in wet conditions: **a** iso $F = 1$ curves for the case study at Cerbaiolo; **b** iso $F = 1$ curves at varying values of non-dimensional group $N = c'/\gamma H$

**Table 4** Parametric study: summary of stability analyses

| Analises in static conditions | | | | | | Analises in seismic conditions | | | | | |
|---|---|---|---|---|---|---|---|---|---|---|---|
| $H$ (m) | $\phi$ (°) | $c$ (kPa) | $\psi_p$ (°) | $z/H$ (–) | $F_{min}$ (–) | $H$ (m) | $\phi$ (°) | $c$ (kPa) | $\psi_p$ (°) | $z/H$ (–) | $F_{min}$ (–) |
| 3 | 25 | 50 | 41.759 | 0.603 | 2.940 | 3 | 25 | 50 | 40.005 | 0.615 | 2.584 |
| | | 30 | 44.159 | 0.586 | 1.964 | | | 30 | 42.689 | 0.597 | 1.732 |
| | | 10 | 51.387 | 0.530 | 0.933 | | | 10 | 50.595 | 0.537 | 0.825 |
| | 30 | 50 | 42.680 | 0.597 | 3.063 | | 30 | 50 | 41.039 | 0.608 | 2.696 |
| | | 30 | 45.362 | 0.577 | 2.076 | | | 30 | 44.022 | 0.587 | 1.833 |
| | | 10 | 53.008 | 0.516 | 1.019 | | | 10 | 52.336 | 0.522 | 0.900 |
| | 35 | 50 | 43.614 | 0.590 | 3.194 | | 35 | 50 | 42.082 | 0.601 | 2.815 |
| | | 30 | 46.544 | 0.569 | 2.195 | | | 30 | 45.325 | 0.578 | 1.9400 |
| | | 10 | 54.493 | 0.503 | 1.109 | | | 10 | 53.921 | 0.508 | 0.978 |
| 5 | 25 | 50 | 44.159 | 0.586 | 1.964 | 5 | 25 | 50 | 42.689 | 0.597 | 1.732 |
| | | 30 | 47.218 | 0.563 | 1.360 | | | 30 | 46.065 | 0.572 | 1.202 |
| | | 10 | 55.298 | 0.495 | 0.698 | | | 10 | 54.777 | 0.500 | 0.615 |
| | 30 | 50 | 45.362 | 0.577 | 2.076 | | 30 | 50 | 44.022 | 0.587 | 1.833 |
| | | 30 | 48.668 | 0.552 | 1.460 | | | 30 | 47.649 | 0.560 | 1.292 |
| | | 10 | 56.939 | 0.480 | 0.772 | | | 10 | 56.516 | 0.484 | 0.679 |
| | 35 | 50 | 46.544 | 0.569 | 2.195 | | 35 | 50 | 45.325 | 0.578 | 1.938 |
| | | 30 | 50.046 | 0.541 | 1.566 | | | 30 | 49.146 | 0.548 | 1.385 |
| | | 10 | 58.402 | 0.465 | 0.850 | | | 10 | 58.056 | 0.468 | 0.745 |
| 8 | 25 | 50 | 46.951 | 0.566 | 1.399 | 8 | 25 | 50 | 45.772 | 0.574 | 1.236 |
| | | 30 | 50.511 | 0.537 | 1.002 | | | 30 | 49.649 | 0.544 | 0.887 |
| | | 10 | 58.877 | 0.460 | 0.549 | | | 10 | 58.554 | 0.463 | 0.481 |
| | 30 | 50 | 48.384 | 0.554 | 1.500 | | 30 | 50 | 47.340 | 0.563 | 1.326 |
| | | 30 | 52.110 | 0.524 | 1.091 | | | 30 | 51.373 | 0.530 | 0.965 |
| | | 10 | 60.443 | 0.442 | 0.614 | | | 10 | 60.193 | 0.445 | 0.535 |
| | 35 | 50 | 49.750 | 0.544 | 1.606 | | 35 | 50 | 48.825 | 0.551 | 1.421 |
| | | 30 | 53.585 | 0.511 | 1.184 | | | 30 | 52.953 | 0.517 | 1.046 |
| | | 10 | 61.809 | 0.426 | 0.681 | | | 10 | 61.615 | 0.429 | 0.592 |

The investigation of the causes and possible solutions to reduce the risk is necessarily multidisciplinary. Starting from a deep knowledge of the historical sequence of events that affected the buildings, an analysis of the geomorphological and geological boundary conditions is required.

In the paper, the case history of the heritage of Cerbaiolo (Tuscany, central Italy) is investigated. The heritage is located on the edge of a terrace along a rock cliff overlapped to a clayey formation. The cliff is affected by numerous and extended fractures in particular along the limits of the rock plate. Moreover, the contrast between the two lithological complexes induces frequent landslides, in particular along the southern boundary where the buildings are placed.

Falls, toppling and slides are the first cause for risk conditions. Moreover, the area belongs to a seismic zone, and the seismic activity acts as an additional predisposing factor for natural hazard. Several parts of the buildings show the proof of the damages caused by gravitational movements.

The geomorphological investigation started from a LiDAR DEM with a spatial resolution of 10 × 10 m. Because of the high resolution of the data, the terrain analysis allowed for the identification of the morphometric and morphological areas where the potential instability is higher. Furthermore, LiDAR data allowed us to obtain a detailed geomorphological map of the transition area between the two lithological complexes, thus highlighting the source areas for mass movements and the free blocks that are slowly moving downstream.

As a second step, a structural-geological survey was carried out along four stations. The collected data allowed for the detection of four main families of discontinuities. Additional information about the type of discontinuity and their orientation, spacing, persistence, roughness, aperture, filling has been obtained. The rock mass was characterized according to Barton et al. (1974); Bieniawski (1989) and Marinos and Hoek (2000).

Results obtained from all the used approaches indicate that the rock mass appears to have a quality from poor to

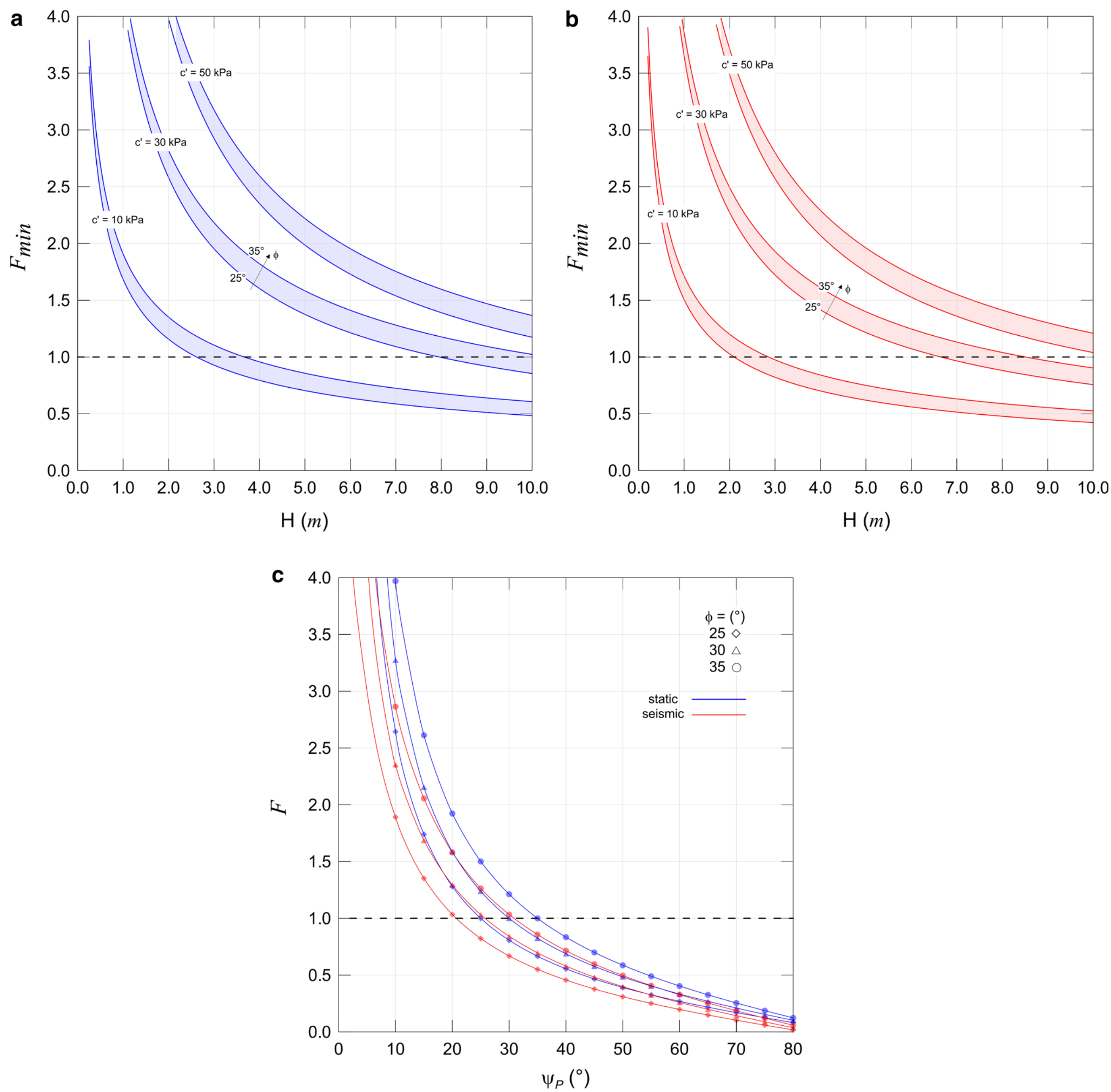


**Fig. 7** $F_{min}$ vs. rock slope height at varying values of $\phi'$, $c'$: **a** static case; **b** seismic condition. **c** $F_{min}$ vs. dip failure plane $\psi_p$ at varying values of $\phi'$ ($c' = 0$) in both static and seismic conditions

fair. The presence of discontinuities allows for the identification of the source areas of landslides. The observations about the presence/absence of filling deposits and water within the fractures, confirm that groundwater plays a major role in the stability conditions along the contact between the hard rock plate and the soft clayey formation.

Finally, the results of the stability analyses in plane failure conditions are presented. The analyses were performed for different hydraulic conditions, in both static and seismic cases. For a "dry slope", the safety factor was minimized regarding the depth of the tension crack and the dip of the slip surface. The effects of rock mass geometry and shear strength parameters of the filling material along the joint surface on the slope stability conditions have been evaluated through a parametric study involving a large number of stability analyses, in both static and seismic cases. The results of such analyses are presented in terms of non-dimensional groups, so that they can be used to find

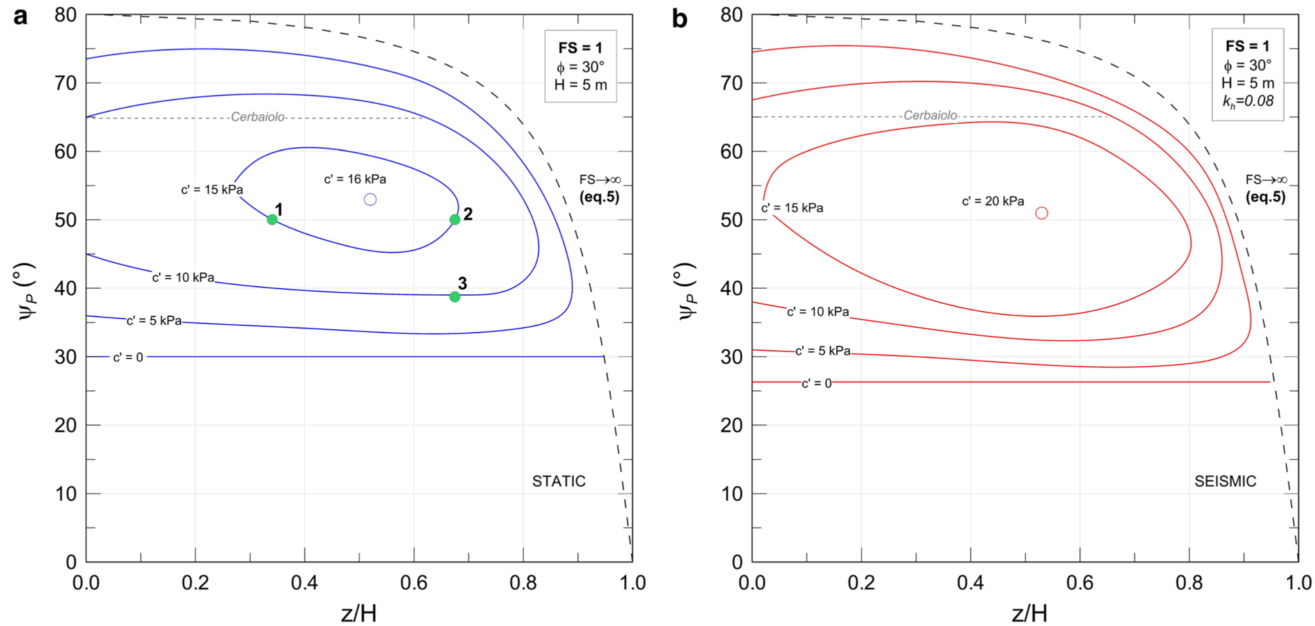


**Fig. 8** Case study of Cerbaiolo: *iso-F* = 1 contours for increasing values of cohesion; **a** static case, **b** seismic case

the best solution for the problem, in terms of safety factor, for a broad range of values of geometrical and mechanical parameters.

The results confirm a widespread instability condition. Landslides and mass wasting show different characteristics along the edge of the cliff, where the dip slope direction, the attitude and type of discontinuities, and the local variation in composition influence the hazard assessment.

## References

Barton NR, Lien R, Lunde J (1974) Engineering classification of rock masses for the design of tunnel support. Rock Mech 6(4):189–239

Bednarczyk Z (2015) Preservation of Saint John Chapel in Dukla from landslide natural hazard. Eng Geol Soc Territ 8:369–374

Benedetti G, Bernardi M, Bonaga G, Borgatti L, Continelli F, Ghirotti M, Marchi G (2013) San Leo: centuries of coexistence with landslides. Landslide science and practice. Springer, Berlin, pp 529–537

Bettelli G, Panini F (1991) Liguridi, mélanges e tettoniti nel Complesso caotico lungo la "Linea del Sillaro" (Appennino settentrionale, Provincie di Firenze e Bologna). Memorie Descrittive della Carta Geologica D'Italia 46:387–415

Bieniawski ZT (1989) Engineering rock mass classifications. Wiley, New York, p 251

Borgatti L, Tosatti G (2010) Slope instability processes affecting the Pietra di Bismantova Geosite (Northern Apennines, Italy). Geoheritage 2:155–168. doi:10.1007/s12371-010-0023-8

Bortolotti V (1962) Stratigrafia e tettonica dei terreni alloctoni (ofioliti e alberese) nei dintorni di Pieve S. Stefano (Arezzo). Bollettino della Società Geologica Italiana 81(3):257–306

Bortolotti V, Mannori G, Principi G, Sani F (2008) Note illustrative della Carta Geologica d'Italia alla scala 1:50.000. Foglio 278 "Pieve Santo Stefano". APAT, Roma

Bozzano F, Bretschneider A, Esposito C, Martino S, Prestininzi A, Scarascia Mugnozza G (2013) Lateral spreading processes in mountain ranges: insights from an analogue modelling experiment. Tectonophysics 605:88–95

Candio S, Cattuto C, Cencetti C, Gregori L, Melelli L (2000) Fenomeni gravitativi intorno alla rupe dell'eremo di Cerbaiolo (Provincia di Arezzo, Toscana orientale): caratterizzazione dell'ammasso roccioso, verifica della stabilità e ipotesi di consolidamento. Atti del Convegno "Condizionamenti Geologici e Geotecnici nella Conservazione del Patrimonio Storico e Culturale" (a cura di G. Lollino), 333–341; Torino, Castello di Moncalieri, 8/9 giugno 2000. Pubblicazione GNDCI-CNR n. 2133

Canuti P, Casagli N, Garzonio CA (1993) Slope instability at a historical site, La Verna Monastery, Italy. Landslide News 7:11–14

Canuti P, Margottini C, Mucho R, Casagli N, Delmonaco G, Ferretti A, Lollino G, Puglisi C, Tarchi D (2005) Preliminary remarks on monitoring, geomorphological evolution and slope stability of Inca Citadel of Machu Picchu. Landslides C101–1:39–47

Casagli N, Fanti R, Nocentini M, Righini G (2005) Assessing the capabilities of VHR satellite data for debris flow mapping in the Machu Picchu area (C101-1). Proceedings ICL General Assembly, Washington D.C. (12–14 October 2005), 61–70

Cecconi M, Viggiani G (2000) Stability of sub-vertical cuts in pyroclastic deposits. In: Proceedings of GeoEng 2000—international conference on geotechnical and geological engineering (Melbourne, 19–24 November 2000), 1–7

Cerrina Feroni A, Martelli L, Martinelli P, Ottria G con contributi di Catanzariti R (2002) Carta geologico-strutturale dell'Appennino emiliano-romagnolo in scala 1:250.000. Regione Emilia Romagna—C.N.R.—I.G.G., Pisa, SELCA, Firenze

D'Amato Avanzi G, Marchetti D, Puccinelli A (2006) Cultural heritage and geological hazards: the case of the Calomini

hermitage in Tuscany (Italy). Landslides 3:331–340. doi:10.1007/s10346-006-0061-0
Delle Donne D, Piccardi L, Odum JK, Stephenson WJ, Williams RA (2007) High-resolution shallow reflection seismic image and surface evidence of the Upper Tiber Basin active faults (Northern Apennines, Italy). Bollettino della Società Geologica Italiana 126:323–331
Dramis F, Sorriso-Valvo M (1994) Deep-seated gravitational slope deformations, related landslides and tectonics. Eng Geol 38(3):231–243
Fanti R, Gigli G, Tapete D, Mugnai F, Casagli N (2013) Monitoring and modelling slope instability in cultural heritage sites. In: Margottini C, Canuti P, Sassa K (eds) Landslide science and practice. Springer, Berlin, Heidelberg, pp 467–473
ISRM (1993) Metodologie per la descrizione quantitativa delle discontinuità nelle masse rocciose. Rivista Italiana di Geotecnica 2:151–197
Laskowicz I, Mrozek T (2015) Sacred historical heritage affected by landslides in the Polish Flysch Carpathians. Eng Geol Soc Territ 8:415–419
Lollino P, Pagliarulo R (2008) The interplay of erosion, instability processes and cultural heritage at San Nicola island (Tremiti archipelago, southern Italy). Geografia Fisica e Dinamica Quaternaria 31:161–169
Margottini C (2001) Instability and geotechnical problems of the Buddha niches and surrounding cliff in Bamiyan Valley, central Afghanistan. Landslides 1(1):41–51
Margottini C, Spizzichino D, Sonnessa A, Puzzilli LM (2015) Natural hazard affecting the Katskhi Pillar Monastery (Georgia). Eng Geol Soc Territ 8:393–397
Marinos P, Hoek E (2000) GSI: a geologically friendly tool for rock mass strength estimation. In: Proceedings of GeoEng 2000—international conference on geotechnical and geological engineering (Melbourne, 19–24 November 2000), 1422–1442
Marinos P, Rondoyanni Th (2005) The archaeological site of Delphi, Greece: a site vulnerable to earthquakes, rockfalls and landslides. In: Proceedings of the 1st general assembly of the International Consortium on Landslides. Springer, Kyoto, chap. 31, pp 241–249
Marinos P, Tsiambaos G (2002) Earthquake triggering rock falls affecting historic monuments and a traditional settlement in Skyros Island, Greece. In: Proceedings of the international symposium: landslide risk mitigation and protection of cultural and natural heritage, Kyoto, Japan, 343–346
Marinos P, Kavvadas M, Tsiambaos G, Saroglou H (2002) Rock slope stabilization in Mythimna castle, Lesvos island, Greece. In: Proceedings of 1st European conference on landslides (Prague, 24–26 June 2002), 635–639, Balkema
McCahon I, Hurley A, Skermer N (2001) Aoraki—Mt Cook Village Flood/Debris Flow Hazard Mitigation [online]. In: Engineering and development in hazardous terrain: New Zealand Geotechnical Society 2001 Symposium, Christchurch, August 2001. Wellington, N.Z.: Institution of Professional Engineers New Zealand, 2001: 409–415. Proceedings of Technical Groups; ISSN 0111-9532; Vol. 29 Issue 2
Melelli L (1998) Fenomeni d'instabilità presso l'eremo di Cerbaiolo (Arezzo, Toscana). Geografia Fisica Dinamica Quaternaria 21:139–145
Melelli L, Pucci S, Saccucci L, Mirabella F, Pazzaglia F, Barchi MR (2014) Morphotectonics of the Upper Tiber Valley (Northern Apennines, Italy), through quantitative analysis of drainage and landforms. Rendiconti Lincei. Scienze Fisiche e Naturali 25:129–138. doi:10.1007/s12210-014-0342-9
Nemcok A (1972) Gravitational slope deformation in high mountains. In: Proceedings of 24th international geology congress, Montreal, Sect. 13: 132–141
Nesci O, Savelli D, Diligenti A, Marinangeli D (2005) Geomorphological sites in the northern Marche (Italy). Examples from autochthon anticline ridges and from Val Marecchia allochthon. Il Quat Ital J Quat Sci 18(1):79–91
Ponzana L (1993) Caratteristiche sedimentologiche e petrografiche della Formazione di Monte Morello (Eocene inferiore-medio, Appennino Settentrionale). Bollettino della Società Geologica Italiana 112:201–218
Pucci S, Mirabella F, Pazzaglia F, Barchi MR, Melelli L, Tuccimei P, Soligo M, Saccucci L (2014) Interaction between regional and local tectonic forcing along a complex quaternary extensional basin: Upper Tiber Valley, Northern Apennines, Italy. Quat Sci Rev 102:111–132. doi:10.1016/j.quascirev.2014.08.009
Ribacchi R, Tommasi P (1988) Preservation and protection of the historical town of San Leo (Italy). IAEG international symposium on engineering geology of ancient works, Monuments and Historical Sites (Athens, 19–23 September 1988), 1: 55–64
Sassa K (2004a) The international consortium on landslides. Landslides 1(1):91–94
Sassa K (2004b) The international programme on landslides. Landslides 1(1):95–99
Spizzichino D, Cacace C, Iadanza C, Trigila A (2013) Cultural heritage exposed to landslide and flood risk in Italy. Geophysical Research Abstracts, Vol. 15, EGU2013-11081, EGU General Assembly 2013
Spreafico MC, Franci F, Bitelli G, Girelli VA, Landuzzi A, Lucente CC, Borgatti L (2015) Remote sensing techniques in a multidisciplinary approach for the preservation of cultural heritage sites from natural hazard: the case of Valmarecchia Rock Slabs (RN, Italy). In: Lollino G, Giordan D, Marunteanu C, Christaras B, Yoshinori I, Margottini C (eds) Engineering geology for society and territory—volume 8. Springer, Switzerland, pp 317–321
Taboroff J (2000) Cultural heritage and natural disasters: incentives for risk management and mitigation. In: Kreimer A, Arnold M (eds) Managing disaster risk in emerging economies, chap 7. Disaster risk management series, No. 2. The World Bank Press, New York, 71–79
Tanarro LM, Muñoz J (2012) Rockfalls in the Duratón canyon, central Spain: inventory and statistical analysis. Geomorphology 169–170:17–29
Wyllie DC, Mah CW (2004) Rock slope engineering: civil and mining, 4th Ed. Based on Rock Slope Engineering (third edition, 1981) by Dr Evert Hoek and Dr John Bray Spon Press is an imprint of the Taylor & Francis Group, London and New York. Master e-book ISBN 0-203-49908-5